

#REPLY TO EDITORS COMMENTS (minor revision) MS bgd-12-2745-2015, 'Modelling the climatic drivers determining photosynthesis and carbon allocation in evergreen Mediterranean forests using multiproxy long time series' by Gea-Izquierdo and coauthors.

Dear Editor,

Please see below our response to your comments (in bold). Lines refer to the enclosed version with track-changes (below). We would like to thank you again for kindly handling the manuscript and for your comments.

With kind regards.

Guillermo Gea-Izquierdo and coauthors.

#####

Thank you for contribution to Biogeosciences and for uploading a revised manuscript. I studied your point-by-point response to referee's comments and found that most points were modified appropriately. However, several comments (though not major) were not adequately addressed, and for improving quality, I encourage further refinement for the following points (they are not mandatory but optional).

6th comment of Reviewer #2 (assumption of respiration)

The constant R_d/A_c ratio seems to be oversimplification also for me, because it means that R_d is zero when A_c is zero. Namely, maintenance respiration was neglected. If correct, please discuss potential bias caused by this assumption.

Please, see lines 241-245 where we acknowledge possible limitations of the way we model autotrophic respiration, which, nevertheless, should be much less important in the studied evergreen forests with photosynthetic activity during the whole year than, e.g. in deciduous forests.

7th comment of Reviewer #2 (equation)

I agree with Reviewer #2 that the sub-index (i) is not always necessary.

As stated, we included a subindex (i) for days to indicate that those variables vary at a daily basis and separate them from the fixed parameters (without index) and from those variables varying yearly (which is indicated with (j)). We still believe that this makes clearer the interpretation of the model and it is necessary to better interpret how the different equations apply. If the journal thinks that this notation is not acceptable, we can always remove those indices, of course. Otherwise, if we can keep them, we would like to do it for the reasons just given.

2nd comment of Reviewer #3 (GPP and precipitation)

Here, the Reviewer #3 recommended performing a sensitivity simulation to separate the effect of precipitation variability in a clearer manner. This applies to another minor comment to (previous) pg. 2764 l8.

Please, see new Figure 6 where we include a simulation with precipitation fixed as for the period 1960-1979 (before the decline), to show clearer the influence of precipitation on the GPP decline

10th comment of Reviewer #3 (CO₂ flux or mixing ratio)

Please check not only line 87 but throughout the manuscript (e.g., line 170, 653, and 663).

We have now better checked this point. See that now we quote along the manuscript either “CO₂ flux” or “[CO₂”, which we define in line 52 as the “CO₂ mixing ratio”.

Technical correction

Line 185

(Misson 2004) should be (Misson 2004).

Corrected (line 163)

1 **Modelling the climatic drivers determining photosynthesis and carbon allocation**
2 **in evergreen Mediterranean forests using multiproxy long time series**

3 ^{1,*}Gea-Izquierdo G, ²Guibal F, ³Joffre R, ³Ourcival JM, ⁴Simioni G, ¹Guiot J

4 ¹CEREGE UMR 7330, CNRS/Aix-Marseille Université. Europole de l'Arbois BP 80
5 13545 Aix-en-Provence cedex 4, France. ²IMBE, CNRS /Aix-Marseille Université
6 UMR 7263 Europole de l'Arbois BP 8013545 Aix-en-Provence cedex 4, France. ³Centre
7 d'Ecologie Fonctionnelle et Evolutive CEFE, UMR 5175, CNRS - Université de
8 Montpellier - Université Paul-Valéry Montpellier – EPHE, 1919 Route de Mende,
9 34293 Montpellier Cedex 5, FRANCE. ⁴Ecologie des Forêts Méditerranéennes, INRA
10 UR 629, Domaine Saint Paul, 84914 Avignon Cedex 9, France.

11 * Author for correspondence: gea-izquierdo@cerege.fr

12

13 **Abstract**

14 Climatic drivers limit several important physiological processes involved in
15 ecosystem carbon dynamics including gross primary productivity (GPP) and carbon
16 allocation in vegetation. Climatic variability limits these two processes differently. We
17 developed an existing mechanistic model to analyse photosynthesis and variability in
18 carbon allocation in two evergreen species at two Mediterranean forests. The model was
19 calibrated using a combination of eddy covariance CO₂ flux data, dendrochronological
20 time series of secondary growth and forest inventory data. The model was modified to
21 be climate explicit in the key processes addressing acclimation of photosynthesis and
22 the pattern of C allocation, particularly to water stress. It succeeded to fit both the high-
23 and the low-frequency response of stand GPP and carbon allocation to stem growth.
24 This would support its capability to address both C-source and C-sink limitations.
25 Simulations suggest a decrease in mean stomatal conductance in response to recent

26 enhancement in water stress and an increase in mean annual intrinsic water use
27 efficiency (iWUE) in both species during the last 50 years. However, this was not
28 translated into a parallel increase in ecosystem water use efficiency (WUE). Interannual
29 variability of WUE followed closely that of iWUE at both sites. Nevertheless, long-term
30 decadal variability of WUE followed the long-term decrease in annual GPP matching
31 the local trend in annual precipitation observed since the [late](#) 1970s at one site. In
32 contrast, at the site where long-term precipitation remained stable, GPP and WUE did
33 not show a negative trend and the trees buffered the climatic variability. In our
34 simulations these temporal changes would be related to acclimation processes to climate
35 at the canopy level including modifications in LAI and stomatal conductance, but also
36 partly related to increasing [CO₂] because the model includes biochemical equations
37 where photosynthesis is directly linked to [CO₂]. Long-term trends in GPP did not
38 match those in growth, in agreement with the C-sink hypothesis. There is a great
39 potential to use the model with abundant dendrochronological data and analyse forest
40 performance under climate change. This would help to understand how different
41 interfering environmental factors produce instability in the pattern of carbon allocation,
42 hence the climatic signal expressed in tree-rings.

43

44 **Keywords:** *Pinus halepensis*, *Quercus ilex*, process-based model, dendrochronology,
45 eddy covariance; global change.

47 Global change challenges forest performance because it can enhance forest
48 vulnerability (IPCC 2013). Trees modify multiple mechanisms at different scales to
49 tackle with environmental stress, including changes in photosynthesis and carbon
50 allocation within plants (Breda et al. 2006; Niinemets 2007; Chen et al. 2013). Many
51 factors affect the different physiological processes driving forest performance. Among
52 them, the net effect of rising CO₂ mixing ratio ([CO₂]) and climate change is
53 meaningful to determine the forests' capacity of acclimation to enhanced xericity
54 (Peñuelas et al. 2011; Keenan et al. 2011; Fatichi et al. 2014). Forest process-based
55 models have been developed to mimic these mechanisms. They can include different
56 levels of complexity but generally implement calculations of leaf photosynthesis up-
57 scaled to the canopy and carbon allocated to different plant compartments (Le Roux et
58 al. 2001; Schaefer et al. 2012; De Kauwe et al. 2013). Although there is evidence that
59 the tree performance depends to some extent on stored carbohydrates (Breda et al. 2006;
60 McDowell et al. 2013; Dickman et al. 2014), these models have received some criticism
61 when used to understand plant performance in response to climate change. This is in
62 part because they are C-source oriented, therefore can exhibit certain limitations to
63 represent the C-sink hypothesis (i.e. that growth rates are limited by environmental
64 factors such as water stress, minimum temperature or nutrient availability rather than by
65 carbohydrate availability) and address dysfunctions related to the tree hydraulics
66 (Millard et al. 2007; Breshears et al. 2009; Sala et al 2012; Körner et al. 2013;
67 McDowell et al. 2013; Fatichi et al. 2014).

68 Complex process-based models profit from multiproxy calibration, particularly
69 when such data are applied at different spatio-temporal scales (Peng et al. 2011). The
70 temporal scale can be approached using time growth series of dendrochronological data.

71 However the analysis of the past always adds uncertainties related to the influence of
72 unknown stand conditions to properly scale productivity. Flux data including stand
73 productivity can be estimated using the eddy covariance technique (Baldocchi 2003).
74 These data overcome many of the limitations of dendroecological data (e.g. intra-annual
75 resolution, control of stand conditions and scaling of net productivity) but they lack
76 their spatial and temporal coverage. Thus, CO₂ flux data can be used to implement
77 unbiased models of canopy photosynthesis, and then combined with dendroecological
78 data to study how carbon is allocated to stem growth as a function of environmental
79 forcing (Friedlingstein et al. 1999; Chen et al. 2013, McMurtrie & Dewar 2013).

80 Mechanistic models can be also used to analyse the environmental factors
81 determining instability in the climate-growth response (D'Arrigo et al. 2008). Different
82 process-based models have been applied with dendroecological data used either in
83 forward or inverse mode (see Guiot et al. 2014 for a review). Among these models, the
84 process-based model MAIDEN (Misson 2004) was originally developed using
85 dendroecological data. The model explicitly includes [CO₂] to calculate photosynthesis
86 (hence its influence on carbon allocation) and includes a carbohydrate storage reservoir.
87 The latter being one of its strengths compared to other models (Vaganov et al. 2006;
88 Sala et al. 2012; Guiot et al. 2014). It has been previously employed to analyse growth
89 variability in one temperate and two Mediterranean species (Misson et al. 2004;
90 Gaucherel et al. 2008) and recently on inverse mode (also including C and O stable
91 isotopes) to reconstruct past climate (Boucher et al. 2014). However, it requires further
92 development to ensure that it provides unbiased estimates of forest productivity and
93 assesses uncertainties in the response of trees to climatic variability at a greater spatial
94 scale at the regional level. Particularly, its parameterization would need improvement if

95 the model is applied to assess how climate modulates forest performance and the pattern
96 of C allocation within plants (Niinemets & Valladares 2004; Fatichi et al. 2014).

97 In this study we use multiproxy data to develop a process-based model and
98 investigate how evergreen Mediterranean forests have modified stand photosynthesis
99 and carbon allocation in response to interacting climatic factors and enhanced [CO₂] in
100 the recent past. The first objective was to develop a process-based model based on
101 MAIDEN (Misson 2004). Within the new version of the model, photosynthesis, carbon
102 allocation, canopy turnover and phenology are now calculated using climate explicit
103 functions with a mechanistic basis. The model is adapted to give unbiased estimates of
104 canopy photosynthesis and stem growth using instrumental data. Specifically, within the
105 new model formulation: (1) photosynthesis is penalized by prolonged water stress
106 conditions through reductions in leaf area index (LAI) and maximum photosynthetic
107 capacity; (2) the pattern of carbon allocation is directly determined by soil water content
108 (i.e. water stress) and temperature through nonlinear relationships; (3) these
109 relationships can be contrasting for different phenophases and affect independently
110 photosynthesis and the pattern of C allocation. Once the model was developed, a second
111 objective was to analyse how [CO₂] and climatic variability affect the temporal
112 instability in annual forest productivity, water use efficiency and carbon allocation. We
113 hypothesise that they will exhibit differences in their long-term variability in relation to
114 recent climate change driven by different functional acclimation processes within trees.

115

116

Material and methods

117 *Study sites and climatic data*

118 The study sites were two evergreen Mediterranean monitored forests in Southern
119 France where CO₂, water vapour and energy fluxes are measured using the Eddy

120 covariance technique (Baldocchi 2003). Both sites are included in FLUXNET
121 (<http://fluxnet.ornl.gov/>). The first site Fontblanche (43.2° N, 5.7° E, 420 m) is a mixed
122 stand where *Pinus halepensis* Mill. dominates the open top canopy layer reaching about
123 12 m, *Quercus ilex* L. forms a lower canopy layer reaching about 6 m and there is a
124 sparse shrub understory including *Quercus coccifera* L. (Simioni et al. 2013). The
125 second site, Puechabon (43.4°N, 3.4° E, 270 m), is a dense coppice in which overstory is
126 dominated by *Q. ilex* with density around 6,000 stems/ha (Rambal et al. 2004; Limousin
127 et al. 2012). Both forests grow on rocky and shallow soils with low retention capacity
128 and of Jurassic limestone origin. The climate is Mediterranean, with a water stress
129 period in summer, cold or mild winters and most precipitation occurring between
130 September and May. Meteorological data were obtained from the neighbouring stations
131 of St. Martin de Londres (for Puechabon) and Aubagne (for Fontblanche). According to
132 those data Puechabon is colder and receives more precipitation than Fontblanche (Table
133 1). Meteorological data showed a decrease in total rainfall since the [1970s](#) in Puechabon
134 but no trend in Fontblanche. Both sites exhibit a positive trend in temperatures more
135 evident for the maximum values (Figure A1).

136 We assumed that GPP is driven by the top pine and/or oak layers and that the
137 percentage of LAI related to the understory shrub layer will behave like that of the oak
138 species (evergreen, shrubby). For Fontblanche we considered a maximum leaf area
139 index (LAI_{max}) of $2.2 \text{ m}^2 \cdot \text{m}^{-2}$ ($3 \text{ m}^2 \cdot \text{m}^{-2}$ plant area index, PAI), composed by a 70% of
140 pine and 30% of oak (Simioni et al. 2013). For Puechabon we considered a LAI_{max} of
141 $2.0 \text{ m}^2 \cdot \text{m}^{-2}$ ($2.8 \text{ m}^2 \cdot \text{m}^{-2}$ PAI) monospecific of *Q. ilex* (Baldocchi et al. 2010; Limousin et
142 al. 2012). Specific leaf area (SLA) considered was $0.0045 \text{ m}^2 \cdot \text{g}^{-1}$ for *Q. ilex* and 0.0037
143 $\text{m}^2 \cdot \text{g}^{-1}$ for *P. halepensis*, respectively (Hoff & Rambal 2003; Maseyk et al. 2008).

144

Guillermo Gea Izquierdo 10/5/y 09:06
Supprimé: 1960s

146 *The model*

147 We used MAIDEN (Misson 2004), a stand productivity mechanistic model driven
148 by a number of functions and parameters representing different processes. The model
149 inputs are precipitation, maximum and minimum temperature and [CO₂] with a daily
150 time step. This model has been previously implemented for monospecific forests
151 including two oaks and one pine species using dendroecological chronologies of growth
152 and, when available, stand transpiration estimates from sap-flow sensors (Misson et al.
153 2004; Gaucherel et al. 2008). However, the model has never been compared to actual
154 CO₂ flux data to ensure that it provides unbiased estimates of forest productivity. In this
155 study, the model was further developed to match ground-based observations and
156 generalize model use by modifying the photosynthesis and allocation modules
157 (including the different phenophases) in relation to climatic drivers. To properly scale
158 model outputs and get unbiased estimates of stand productivity we used CO₂ eddy
159 covariance fluxes (Baldocchi 2003). Different parameters were calibrated to different
160 data sources, including some species-dependent and some site-dependent parameters, as
161 follows. The transpiration rate (E) of day *i* is calculated using a conductance approach
162 as $E(i) = g_s(i) \cdot VPD(i) / P_{atm}(i)$, where P_{atm} is atmospheric pressure and g_s and VPD are
163 stomatal conductance and vapour pressure deficit, respectively, as described below
164 (Misson 2004). Those other equations used to calculate micrometeorological covariates,
165 soil humidity and photosynthetic active radiation, as well as those functions describing
166 the water cycle (including soil evaporation and plant transpiration) are explained in the
167 original model formulation from Misson (2004). Therefore they won't be described
168 here. The rest of the model was modified as follows.

169

170 *Modelling the effect of climatic forcing on photosynthesis*

Guillermo Gea Izquierdo 7/5/y 17:11
Mis en forme: Non Exosant/ Indice

Guillermo Gea Izquierdo 7/5/y 17:06
Supprimé: s

172 Leaf photosynthesis (A_n) is calculated based on the biochemical model of Farquhar
 173 et al. (1980). A_n is a function of the carboxylation (V_c), oxygenation (V_o) and leaf dark
 174 respiration rates (R_d): $A_n = V_c - 0.5V_o - R_d$; where photosynthesis at day i is limited by either
 175 the rate of carboxylation when Rubisco is saturated (W_c) or when it is limited by
 176 electron transport (W_j), i.e. $A_c = V_c - 0.5V_o = \min\{W_c, W_j\}$. R_d was considered a fixed
 177 function of A_c ($0.006 \cdot A_c$), because it performed better in our daily model than
 178 exponential formulations as a function of temperature (Sala & Tenhunen 1996; De Pury
 179 & Farquhar 1997; Bernacchi et al. 2001). Following De Pury & Farquhar (1997):

$$W_c(i) = \frac{V_{cmax}(i) \cdot (C_i(i) - \Gamma(i))}{C_i(i) + K_c(i) \left(1 + \frac{[O_2]}{K_o(i)}\right)} \quad [E1],$$

$$W_j(i) = \frac{J_{max}(i) \cdot (C_i(i) - \Gamma(i))}{4C_i(i) + 8\Gamma(i)} \quad [E2];$$

180 where C_i is the CO₂ intercellular concentration, Γ is the [CO₂] compensation point for
 181 photosynthesis in the absence of dark respiration, and K_c and K_o are the kinetic
 182 Michaelis-Menten constants for carboxylation and oxygenation, respectively. V_{cmax} and
 183 J_{max} are temperature dependent parameters as follows. Photosynthesis is known to
 184 respond to the carbon concentration within chloroplasts C_c rather than to C_i . We keep
 185 through the paper the notation presented here in [E1] and [E2] but discuss below how
 186 mesophyll conductance is taken into account empirically in relation to water stress
 187 when calculating g_s and acknowledge the possible limitations of our approach
 188 (Reichstein et al. 2002; Grassi & Magnani 2005; Flexas et al. 2006; Sun et al. 2014).

189 Climate influences leaf photosynthesis calculations through the temperature
 190 dependence of different parameters (Bernacchi et al. 2001; Nobel 2009). Γ , K_c and K_o
 191 were modelled using Arrhenius functions of daily mean temperature (T_{day} , in °C) with
 192 parameters as in De Pury & Farquhar (1997). We modelled J_{max} as a fixed rate of V_{cmax}
 193 ($J_{max}(i) = J_{coef} \cdot V_{cmax}(i)$) after comparing with different temperature dependent

Guillermo Gea Izquierdo 10/5/y 09:21

Supprimé: (i)

Guillermo Gea Izquierdo 10/5/y 09:21

Mis en forme: Indice

195 formulations (De Pury & Farquhar 1997; Maseyk et al. 2008). The model behaviour
 196 was better when the temperature dependence of V_{cmax} was modelled using a logistic
 197 function (Gea-Izquierdo et al. 2010) rather than an exponential function as in Misson
 198 (2004):

$$V_{cmax}(i) = \frac{V_{max}}{(1 + \exp(V_b \cdot ((T_{day}(i) + 273) - V_{ip})))} \cdot \theta_p \quad [E3];$$

199 V_{max} , V_b and V_{ip} are parameters to be estimated, with V_{max} being the asymptote and V_{ip}
 200 the inflection point. θ_p is a soil water stress function dependent on soil moisture
 201 conditions of the previous year. It takes into account down-regulation of photosynthesis
 202 in response to protracted drought through its impact on the photosynthetic capacity of
 203 active LAI in evergreen species caused by constraints in V_{cmax} produced by irreversible
 204 photoinhibition, modifications in leaf stoichiometry and/or aging of standing foliage
 205 through lower leaf replacement rates in response to long-term water stress (Sala &
 206 Tenhunen 1996; Niinemets & Valladares 2004; Niinemets 2007; Vaz et al. 2010).
 207 $\theta_p = 1 - \exp(p_{str} \cdot SWC_{180})$ [E4], where p_{str} is a parameter to be estimated and
 208 SWC_{180} is the mean soil water content (mm) from July to December of the previous
 209 year.

210 Photosynthesis is coupled to stomatal conductance calculation, which is estimated
 211 using a modified version of the Leuning (1995) equation:

$$g_s(i) = \frac{g_1 \cdot A_n(i)}{(C_s(i) - \Gamma(i)) \cdot (1 + VPD(i)/VPD_0)} \cdot \theta_g(i) \quad [E5],$$

212 g_1 and VPD_0 are parameters, $VPD(i)$ is daily vapour pressure deficit, C_s is the leaf
 213 surface [CO_2]; θ_g is a non-linear soil water stress function as:

$$\theta_g(i) = \frac{1}{1 + \exp(soil_b \cdot (SWC(i) - soil_{ip}))} \quad [E6],$$

214 $soil_b$ and $soil_{ip}$ are parameters and $SWC(i)$ is daily soil water content (mm). θ_g accounts
 215 for variability in gas exchange under drought conditions which cannot be taken into
 216 account only through stomatal control, e.g. related to mesophyll conductance or
 217 stomatal patchiness. Therefore, with this empirical expression we partly represent the
 218 effect of CO_2 fractionation during mesophyll conductance under water stress,
 219 acknowledging that this will be likely more complex under environmental stress
 220 (Reichstein et al. 2002; Grassi & Magnani 2005; Flexas et al. 2006; Sun et al. 2014).
 221 The coupled photosynthesis-stomatal conductance system of equations was estimated
 222 separately for sun and shade leaves. Canopy photosynthesis was integrated using LAI
 223 divided into its sunlit and shaded fractions (De Pury & Farquhar 1997). Transmission
 224 and absorption of irradiance was calculated following the Beer-Lambert law as a
 225 function of LAI, with $LAI_{sun}=(1-\exp(-LAI))\cdot K_b$ (K_b is the beam light extinction
 226 coefficient, which was set to 0.8) and $LAI_{shade}=LAI-LAI_{sun}$ (Misson 2004). In the mixed
 227 stand (Fontblanche), photosynthesis was calculated separately for *Q. ilex* and *P.*
 228 *halepensis*, and then integrated to get stand estimates of forest productivity.

229

230 *Modelling the effect of climatic forcing on carbon allocation*

231 The model allocates daily carbon assimilated either to the canopy, stem, roots or
 232 storage of non-structural carbohydrates (NSC) to mimic intra-annual carbohydrate
 233 dynamics (Misson 2004; Dickman et al. 2014). Although trees can store carbon within
 234 different above-ground and below-ground compartments (Millard et al. 2007), carbon
 235 storage is treated as a single pool within the model. Tree autotrophic respiration ($R_{a, in}$
 236 addition to R_d) is modelled as a function $f(i)$ of daily photosynthesis and maximum daily
 237 temperature (T_{max}) (Sala & Tenhunen 1996; Nobel 2009) as:

238 $R_a(i) = A_n(i) \cdot \max\{0.3, f(i)\}$, with $f(i) = 0.47 \cdot (1 - \exp(p_{respi} \cdot T_{max}(i)))$ [E7];

Guillermo Gea Izquierdo 7/5/y 18:11
 Mis en forme: Non Exosant/ Indice
 Guillermo Gea Izquierdo 7/5/y 18:11
 Mis en forme: Police :Non Italique, Non Exosant/ Indice

Guillermo Gea Izquierdo 10/5/y 09:35
 Supprimé: $A_n(i)$.

240 where p_{respi} is a parameter. Net photosynthesis is calculated for day i as $A_N(i) = A_n(i) -$
241 $R_d(i)$. [This assumption means that respiration would be considered nil when there is no](#)
242 [photosynthesis, hence maintenance respiration would not be taken into account those](#)
243 [days. Although this could bias the overall carbon balance, we assume that this effect](#)
244 [will be very reduced in the studied forests because they present photosynthetic activity](#)
245 [all year round \(see results\).](#) The model simulates several phenological phases during the
246 year (see Figure 1):

247 [P1] winter period where all photosynthates assimilated daily, $A_N(i)$, are allocated to the
248 storage reservoir (NSCs) but there is no accumulation of growing degree days (GDD).

249 [P2] winter period where all $A_N(i)$ are allocated to storage (i.e. the same as in [P1]) but
250 in opposition to [P1] there is active accumulation of GDD which define the threshold
251 GDD_t to trigger the next phenophase [P3] (budburst, leaf-flush).

252 [P3] budburst, where carbon available $C_T(i) = A_N(i) + C_{bud}$ (C_{bud} is daily C storage utilized
253 from buds, a parameter) is either allocated to the canopy, to roots or to the stem.

254 [P4] once the canopy has been completed in [P3], the next phenophase [P4] starts; in
255 this period, daily photosynthates $A_N(i)$ are allocated either to the stem or to storage;

256 [P5] the last phenophase [P5] starts when the photoperiod (parameter) crosses a
257 minimum threshold in fall. In this phase root mortality occurs. Otherwise [P5] is similar
258 to [P1] and [P2], in the sense that all $A_N(i)$ is used for storage until next year [P3] starts.

259 Allocation of carbon to different plant compartments is complex because it can be
260 decoupled from photosynthetic production depending on different factors, some of them
261 climatic, acting at different temporal scales (Friedlingstein et al. 1999; Sala et al. 2012;
262 Chen et al. 2013; McMurtrie & Dewar 2013). In this new version of the model we set
263 the different allocation relationships as nonlinear functions of temperature and soil
264 water content, $h(i) = f_1(T_{max}) \cdot f_2(SWC)$, in [P3] and [P4] following the functional

265 relationships described in Gea-Izquierdo et al. (2013). This means that now we take into
 266 account homeostatic acclimation processes at the canopy level related to LAI
 267 dependence on water availability (Hoff & Rambal 1993; Sala & Tenhunen 1996;
 268 Reichstein et al. 2003). LAI is negatively related to long-term drought because litterfall
 269 is negatively linked to water stress (Limousin et al. 2009; Misson et al. 2011) and bud
 270 size depends on climate influencing the period of bud formation (Montserrat-Marti et al
 271 | 2009). Therefore the actual carbon that can be allocated to the canopy in [P3] of year j
 272 ($AlloC_{canopy}(j)$) was set as a function of previous year moisture conditions ($\theta_{LAI}(j)$), and
 273 maximum carbon that can be allocated to the canopy ($MaxC_{canopy}$). $MaxC_{canopy}$ is
 274 calculated from LAI_{max} and SLA , and $AlloC_{canopy}(j) = \theta_{LAI}(j) \cdot MaxC_{canopy}$, where:
 275 $\theta_{LAI}(j) = \left(1 - 2 \cdot \frac{p_{LAI} - SWC_{250}}{p_{LAI}}\right)$, constrained to $\theta_{LAI}(j) \in [0.7, 1.0]$ [E8]
 276 p_{LAI} is a parameter to be calibrated representing the threshold over which $\theta_{LAI}(j) = 1$
 277 and SWC_{250} is mean soil water content for May-December of previous year.

278 Leaf turnover is variable within years and partly related to water availability
 279 (Limousin et al. 2009, 2012). We considered a mean leaf turnover rate of 3 years for
 280 pines and 2 for oaks. To model within year variability in leaf phenology (i.e. leaf
 281 growth and litterfall) we followed Maseyk et al. (2008) and Limousin et al. (2009)
 282 (Figure 1). C allocation to the canopy (i.e. including primary growth) in [P3] is
 283 | calculated as: $C_{canopy}(i) = C_T(i) \cdot (1 - 0.2 \cdot h_{3_1}(i)) \cdot Ratio_{root/leaf}^{-1}$; $Ratio_{root/leaf}$ was fixed to 1.5
 284 for both species (Misson et al. 2004; Ourcival, unpublished data), and:

$$h_{3_1}(i) = \left(1 - \exp(p_{3moist} \cdot SWC(i)) \cdot \exp\left(-0.5 \cdot \left(\frac{T_{max}(i) - p_{3temp}}{p_{3sd}}\right)^2\right)\right) \quad [E9],$$

285 p_{3moist} , p_{3temp} and p_{3sd} are parameters representing the scale of the SWC and the optimum
 286 and dispersion of the T_{max} functions respectively. The carbon allocated to the stem
 287 (C_{stem}) in [P3] is $C_{stem}(i) = C_T(i) \cdot 0.2 \cdot h_{3_1}(i) \cdot h_{3_2}(i)$, where:

Guillermo Gea Izquierdo 10/5/y 09:47
 Mis en forme: Police :Italique

Guillermo Gea Izquierdo 10/5/y 10:09
 Mis en forme: Expositant

288
$$h_{3_2}(i) = (1 - \exp(st_{3moist} \cdot SWC(i)) \cdot \left(\exp\left(-0.5 \cdot \left(\frac{T_{max}(i) - st_{3temp}}{st_{3sd_temp}}\right)^2\right)\right)) \quad [E10];$$

289 with $h_{3_1}(i)$ as in [E9]; st_{3moist} , st_{3temp} and st_{3sd_temp} are parameters as in $h_{3_1}(i)$. The
 290 carbon allocated to roots in [P3] is set complementary to that of the other compartments
 291 to close the carbon budget within the tree, i.e.: $C_{roots}(i) = C_T(i) - C_{stem}(i) - C_{canopy}(i)$.

292 Finally, in [P4] carbon assimilated daily $A_N(i)$ is allocated either to stem growth or
 293 to storage until changing to [P5]. There since in [P1] and [P2] again all $A_N(i)$ is only
 294 allocated to storage until [P3] next year (Misson 2004). In [P4], the amount of carbon to
 295 be allocated to stem growth is now also set as a function of climatic forcing:

296 $C_{stem}(i) = A_N(i) \cdot (1 - h_4(i))$ and $C_{stor}(i) = A_N(i) \cdot h_4(i)$, with:

297
$$h_4(i) = (1 - \exp(st_{4temp} \cdot T_{max}(i)) \cdot \left(\exp\left(-0.5 \cdot \left(\frac{SWC(i)}{st_{4sd_moist}}\right)^2\right)\right)) \quad [E11];$$

298 st_{4temp} and st_{4sd_temp} are parameters as from [E10].

299

300 *Eddy covariance CO₂ flux and dendrochronological data*

301 The process-based model was calibrated using daily gross primary productivity
 302 (GPP), dendrochronological data and inventory data. To develop the model, in a first
 303 step those functions used to model daily stand photosynthesis (i.e. [E1] to [E9]) were
 304 calibrated against GPP values. GPP estimates were obtained from half-hourly net CO₂
 305 flux measurements (NEP). GPP was obtained as the difference between measured net
 306 ecosystem productivity and calculated ecosystem respiration (Reichstein et al. 2005).
 307 Negative GPP values were corrected following Schaefer et al. (2012). Half-hourly GPP
 308 data were integrated to obtain daily estimates for the period 2001-2013 (Puechabon,
 309 methods detailed in Allard et al. (2008)) and 2008-2012 (Fontblanche) (Table 1).

310 In a second step, those functions used to model how carbon assimilated and/or
 311 storage is allocated to growth of the tree stem (i.e. [E10] and [E11]) were developed

312 using calculated annual stem biomass increment time series. Stem biomass increment
313 chronologies were built combining dendroecological data and forest inventory data
314 collected at each site. We built one chronology for *Q. ilex* in Puechabon, a second for *Q.*
315 *ilex* in Fontblanche and a third one for *P. halepensis* at Fontblanche (Figure 2). For
316 pines, two perpendicular cores were extracted using an increment borer from 25 trees in
317 fall 2013 whereas for oaks we used crosssections. In Fontblanche, 15 oak stems were
318 felled and basal sections collected in spring 2014. A total of 17 oak stems from
319 Puechabon were logged in 2005 and 2008. The age and diameter distributions of the
320 studied forests are depicted in Figure A2.

321 All samples were processed using standard dendrochronological methods (Fritts
322 1976). Annual growth (RW) was measured using a stereomicroscope and a moving
323 table switched to a computer. RW crossdating was visually and statistically verified.
324 RW estimates were transformed to basal area increments (BAI, $\text{cm}^2 \cdot \text{year}^{-1}$). Mean BAI
325 chronologies were obtained by averaging individual tree BAI time series. In
326 Fontblanche BAI during the period 1987-1995 was standardized relative to the mean
327 calculated after excluding that period (Figure 2). BAI data were standardized because
328 we did not find a climatic explanation for the abrupt growth peak observed in
329 Fontblanche during that period (Figure 2). Therefore we assumed that it had been
330 caused by a release event (i.e. reduction in competition) produced by the death of
331 neighbours as a consequence of winter frost during 1985 and 1987 (Vennetier, pers.
332 comm., 2014). These two frosts were reflected by the presence of characteristic frost
333 rings in most individuals from Fontblanche.

334 To scale BAI chronologies to the same units as annual stem biomass (which is an
335 output of the model) we used plot inventory data collected around the flux towers at the
336 two sites. Inventory data included stem diameter for all trees and tree height collected

337 for a subsample every two years during 2007-2011 in Fontblanche, and annual diameter
338 estimates for the period 1986-2011 for Puechabon. Individual annual biomass
339 increments were estimated by subtracting stem biomass at consecutive years and then
340 stand stem biomass increment (SBI, $\text{g C m}^{-2}\cdot\text{year}^{-1}$) built integrating plot data. Stem
341 biomass was calculated using allometric functions. For pines, we calculated stem
342 biomass using diameter and estimated stem height assuming that the tree bole follows a
343 paraboloid shape (Li et al. 2014). For oaks, stem biomass was calculated following
344 Rambal et al. (2004). Once SBI had been estimated for the years when we had available
345 inventory data, BAI chronologies were correlatively scaled to SBI units ($\text{g C m}^{-2}\cdot\text{year}^{-1}$).
346 We built two mean stand SBI chronologies, one for each site, meaning that we
347 analysed carbon allocation within stands, not differentiating between species in
348 Fontblanche. These two SBI chronologies were used to calibrate sitewise [E10] and
349 [E11].

350

351 *Model development and analyses*

352 Parameters were selected according to the ecological characteristics of the species,
353 exploring the model using comprehensive sensitivity analysis to sequentially optimize
354 groups of parameters. In a first step, a group of common parameters (those included in
355 [E2] to [E8]) was selected using GPP data from Fontblanche (Table 2). The species-
356 dependent parameters selected for *Q. ilex* in this first step were independently validated
357 when applied in Puechabon (those in Table 2 common for the two sites). In a second
358 step, a subset of site-dependent parameters was calibrated against GPP and SBI data.
359 Four from [E6] and [E9] were calibrated using GPP data, and five parameters in [E10]
360 and [E11] were calibrated using stem biomass increment data (Table 2). The local

361 parameters were calibrated constrained to an ecologically realistic range using a global
362 optimization algorithm and maximum likelihood principles (Gaucherel et al. 2008).

363 To compare model output with stem biomass chronologies as estimated from
364 dendroecological data we used only the period where we had available daily
365 meteorological data (1960-2013), which was also a period that did not include juvenile
366 years with increasing BAI (BAIs reached an asymptote after increasing the first 15-20
367 juvenile years, Figure 2). The model does not take into account how size differences in
368 allometry or ontogeny affect carbon allocation (Chen et al. 2013). We tried to keep the
369 model as simple as possible also because we had no such data to calibrate ontogenic
370 effects. Hence the model is designed for non-juvenile stands with canopies that reached
371 a steady state with asymptotic LAI_{max} . For the same reasons it does not take into account
372 how changes in management affect carbon allocation. The model was analysed in terms
373 of goodness of fit. Additionally, for the period where we had available daily
374 meteorological data we simulated time series of GPP, ecosystem water use efficiency
375 ($WUE = GPP/ET$, with ET =actual evapotranspiration) and intrinsic water use
376 efficiency of sun leaves ($iWUE = A_N/g_s$) calculated following Beer et al. (2009).

377

378

Results

379 The studied evergreen forests exhibit a bimodal pattern in GPP with maxima in
380 spring and autumn (Figure 3) as often observed in Mediterranean ecosystems (e.g.
381 Baldocchi et al. 2010). GPP was above zero almost every day of the year, including
382 winter, particularly in the milder site, Fontblanche (Table 1). This means that there is
383 active photosynthesis all year round in these evergreen forests, including both periods of
384 climatic stress with low temperature and short photoperiod in winter, and with low
385 moisture availability in summer (Figure 3). Mean annual GPP was 1431.4 ± 305.4 g C m⁻²

Guillermo Gea Izquierdo 10/5/y 10:24
Mis en forme: Police :Italique

386 $\text{g C m}^{-2} \text{ year}^{-1}$ and precipitation 642.7 ± 169.7 mm in Fontblanche; whereas it was 1207.3 ± 206.7
387 $\text{g C m}^{-2} \text{ year}^{-1}$ and 1002.6 ± 328.2 mm in Puechabon (see Table 1 for more details). Mean
388 GPP was higher at Fontblanche because carbon assimilation was greater in the low
389 temperature winter period but similar the rest of the year (Figure 3). Stem growth did
390 not show any long-term (decadal) growth trend for any of the species studied (Figure 2).

391 The model accurately represented the low frequency response of GPP: both the
392 seasonal variability in GPP within years and variability in GPP among years (Figure 4).
393 The model explained over 50% of the annual biomass growth variance, and 46% and
394 59% of daily GPP in Fontblanche and Puechabon, respectively (Figure 4). This means
395 that we were able to mimic the daily, seasonal and long-term trends in stand
396 productivity with unbiased estimates but also to model how carbon is allocated to stem
397 growth along the year at the different phenophases described. The model assumed
398 species-specific carbon allocation responses set to the different plant compartments as
399 nonlinear functions of temperature and soil moisture. These relationships were
400 biologically meaningful in the sense that photosynthesis and carbon allocation could be
401 decoupled to some extent as a function of climatic variability. Once the canopy has been
402 formed in spring, the model allocated more carbon to the stem and less to storage when
403 less severe [climatic](#) stress occurs, i.e. with decreasing temperatures and more humid
404 conditions (Figure 5).

405 Both sites exhibited an increase in temperature particularly evident in the maximum
406 values but only Puechabon suffered a decrease in annual precipitation between 1960 and
407 2012 (Figure A1). In the model, the studied forests acclimated to changing climatic
408 conditions in the last decades coupling different physiological traits and simulated
409 annual GPP greatly followed the overall trends in precipitation observed. In
410 Fontblanche, which is milder and receives less precipitation, GPP remained stable since

411 the 1960s and presented no apparent long-term trend (Figure 6). In contrast, in the
412 coldest and rainiest site (Puechabon) the model simulated a decrease in GPP (Figure 6),
413 which was driven by the prevailing decrease in precipitation observed since the 1970s
414 (Figure A1; Figure 6). This reduction of GPP was partly a consequence of decreased
415 LAI in response to enhanced long-term water stress (Figure A3; Limousin et al. 2009;
416 Misson et al. 2011). Simulated long-term decadal trends in mean annual stomatal
417 conductance were similar and decreasing at the two sites with greater water stress as a
418 consequence of enhanced temperatures (Figure 6). The two species studied showed a
419 long-term increase in simulated iWUE (Figure 7) following the decrease in simulated g_s
420 (Figure 6). The interannual variability of WUE and iWUE were highly and positively
421 correlated (Figure 7). However, in the long-term they followed a different pattern
422 particularly in Puechabon where there was a recent decline in WUE (not observed in
423 iWUE) forced by trends in ET and GPP (Figure 7). This means that the recent reduction
424 in simulated GPP was proportionally greater than that of simulated ET (Figure 6; Figure
425 A3).

426

427

Discussion

428 *Linking photosynthetic production to carbon allocation as a function of climate*

429 The model calculates stand productivity and carbon allocation to stem growth in
430 response to climate and $[CO_2]$ with realism. It is particularly well suited to mimic the
431 effect of water stress in plant performance by the explicit assessment of different
432 acclimation processes at the canopy level including changes in stomatal conductance
433 and photosynthetic capacity (Sala & Tenhunen 1996; Reichstein et al. 2003; Limousin
434 et al. 2010; Misson et al. 2011). Additionally, the model simulates carbohydrate storage
435 dynamically as a function of environmental variability. Climate can affect differently

Guillermo Gea Izquierdo 10/5/y 09:07

Supprimé: 1960s

437 the carbon dynamics and pattern of C-allocation to different tree compartments at
438 different phenophases. In the model the storage reservoir is an active sink for
439 assimilated carbon during some periods of the year and a source in spring to be used in
440 primary and secondary growth (Figure A5). Additionally stem growth is limited by
441 climatic constraints (in [P3] and [P4]) rather than just by the amount of available
442 carbohydrates (Millard et al. 2007). This means that water stress and optimum
443 temperature directly affect the modelled processes assuming that cell-wall expansion in
444 the xylem can relate to climatic variability differently than photosynthetic production
445 (Sala et al. 2012). The model showed C-limitation (for primary growth) the years when
446 LAI_{max} was not achieved (i.e. a limitation in LAI is driven by limitations in the C supply
447 in spring), e.g. all years in Puechabon for the period shown in Figure A5 (1995-2012)
448 but only those years in Fontblanche when the minimum value considered as a threshold
449 was reached. Therefore both C-source (photosynthesis) and C-sink (just related to
450 growth, other sinks such as volatile organic compounds or root exudates are not
451 explicitly included in the model) limitations can be assessed at different years within
452 one site and even at different periods within the same year (Millard et al. 2007; Sala et
453 al. 2012; Chen et al. 2013; Fatichi et al. 2014). This hypothesis seems plausible as
454 drought stress affects both C-source (e.g. through reduced stomatal conductance) and C-
455 sink limitations (e.g. cell water turgor, hydraulic performance) (McDowell et al. 2013).
456 Whether the pattern of C-storage simulated is realistic is something that needs to be
457 validated against actual data. However, the flexible way in which stored C is modelled
458 has much potentiality to improve ecosystem models that only view a carbon-source
459 limitation (Sala et al. 2012; Friend et al. 2014).

460 Water stress is generally considered the greatest limitation for Mediterranean
461 ecosystems, driving an intimate relation between precipitation and both growth and

462 photosynthesis (Breda et al. 2006; Pereira et al. 2007; Baldocchi et al. 2010; Gea-
463 Izquierdo & Cañellas 2014). Our results show that a long-term decrease in precipitation
464 triggered a decrease in simulated GPP at the more rainy and coldest site. However, this
465 decline was not expressed in the growth-trends. This means that long-term productivity
466 and allocation of C to secondary growth were decoupled and did not match (Sala et al.
467 2012; Chen et al. 2013; Fatichi et al. 2014). The existence of trade-offs between carbon
468 assimilation and allocation in relation to environmental variability suggests caution
469 when using growth as a direct proxy to investigate stand productivity dynamics (e.g.
470 Piovesan et al. 2008; Peñuelas et al. 2008; Gea-Izquierdo & Cañellas 2014). GPP was
471 greater in the site receiving less precipitation, which could be related to differences in
472 soil retention capacity. However both soils are calcareous, shallow and stony and
473 differences in GPP were greatly explained by less limitation for carbon assimilation of
474 low winter temperatures at the warmest site (Fontblanche). They can also be a result of
475 different species composition (oak vs. pine-oak). LAI is greater at the site yielding
476 higher annual GPP. Nonetheless, had this factor been responsible for the observed
477 differences in winter photosynthesis, there would have also been differences in spring
478 photosynthesis, which was not the case (Figure 3).

479 A better understanding of the underlying processes determining carbon allocation
480 will benefice process-based models (Sala et al. 2012; Fatichi et al. 2014). Model
481 parameters were within the range found in the literature, bearing in mind that using a
482 daily time step to study differential processes or not distinguishing between leaf ages
483 will affect the scaling of parameters such as J_{max} , V_{cmax} or R_d (De Pury & Farquhar 1997;
484 Grassi & Magnani 2005; Masseyk et al. 2008; Vaz et al. 2010). Daily climatic data are
485 readily available at a greater spatial scale than data with a higher temporal resolution,
486 which increases applicability of daily models. Model performance could be improved

Guillermo Gea Izquierdo 10/5/y 10:58
Supprimé: continental

Guillermo Gea Izquierdo 10/5/y 11:00
Supprimé: /

489 by addressing respiration changes related to ontogeny and allometry, nutrient limitations
490 (e.g. N/P) on photosynthesis, or including more complex up-scaling of leaf-level
491 photosynthesis (Niinemets et al. 1999; Niinemets 2007; Chen et al. 2013; McMurtrie &
492 Dewar 2013). However, it is difficult to find suitable data to calibrate such processes.
493 Similarly, it would be challenging to include allocation to reproductive effort in the
494 carbon budget. This is because, even if it is influenced by water stress in the studied
495 forests (Pérez-Ramos et al. 2010), there is still great uncertainty in the causal factors
496 driving multi-annual variability in fruit production (Koenig and Knops 2000).
497 Addressing stand dynamics would also help to generalize model applicability. Stand
498 disturbances modifying stand competition can leave an imprint in growth for more than
499 a decade whereas they do not seem to affect stand GPP over more than one or two years
500 if the disturbance is moderate (Misson et al. 2005; Granier et al. 2008). In response to
501 changes in competition the trees modify [the carbon allocation pattern](#) or keep the
502 root:shoot ratio constant to enhance productivity on a per-tree basis but up to an
503 asymptotic stand GPP. Still, the model behaviour was good compared with other studies
504 that addressed ontogenic changes in the carbon-allocation response to photosynthesis
505 (Li et al. 2014) and similar or better than that of other mechanistic approaches calibrated
506 to standardized dendroecological data (Misson et al. 2004; Evans et al. 2006; Gaucherel
507 et al. 2008; Tolwinski-Ward et al. 2011; Touchan et al. 2012).

508

509 *Forest performance in response to recent climate change and [CO₂] enhancement*

510 Few studies under natural conditions observed a net increase of growth rates in
511 response to enhanced [\[CO₂\]](#) levels since the late 1800s, meaning that other factors such
512 as water stress and/or N/P were more limiting for photosynthesis and/or allocation to
513 growth than [CO₂] (Niinemets et al. 1999; Peñuelas et al. 2011; McMurtrie & Dewar

Guillermo Gea Izquierdo 10/5/y 11:03

Supprimé:

Guillermo Gea Izquierdo 7/5/y 17:12

Mis en forme: Non Exposant/ Indice

515 2013; Lévesque et al. 2014). Yet the forests have increased their iWUE. This can be
516 partly a passive consequence of enhanced [CO₂] but higher iWUE observed in more
517 water stressed sites suggests that climate is co-responsible for an active acclimation of
518 physiological plant processes (Keenan et al. 2013; Leonardi et al. 2013; Saurer et al.
519 2014). These processes would include a higher stomatal control like in our results where
520 in turn we did not observe any increase in long-term carbon assimilation. The mean
521 annual stomatal conductance simulated was driven by climate but also decreased
522 simultaneously in time with increasing [CO₂] (Appendix A4). Furthermore, there is
523 debate on whether there has been an increase in ecosystem WUE in response to recent
524 changes in [CO₂] under a warming climate (Beer et al. 2009; Reichstein et al. 2002;
525 Keenan et al. 2013). In our results the high-frequency of WUE followed that of iWUE,
526 but there was some mismatch between the two traits in the low-frequency. We observed
527 [no dominant time trends in](#) simulated annual WUE for the period 1980-2000 at the site
528 where precipitation remained stable, whereas there was a decrease in WUE following
529 that in GPP particularly evident in the site experiencing a drier climate in recent years.
530 This trend was not observed in iWUE, which means that reductions in GPP and g_s were
531 proportionally greater than those in ET (Figure 6, Figure 7, Appendix A3).

532 Higher [CO₂] concentrations enhance photosynthesis with the equations used to
533 calculate leaf photosynthesis in biochemical models (e.g. Gaucherel et al. 2008; Keenan
534 et al. 2011; Leonardi et al. 2013; Boucher et al. 2014). Thus, the absence of a long-term
535 increase in GPP and growth would not mean that enhanced [CO₂] was not beneficial for
536 model outputs (particularly in the case of C-source limitation) but that the net control
537 exerted by other factors such as climatically driven stress was more limiting than that of
538 [CO₂] availability: growth and photosynthesis would have been lower had we used
539 constant [CO₂] with the same model parameters. The absence of any modification in the

Guillermo Gea Izquierdo 10/5/y 11:25

Supprimé: an increase in

Guillermo Gea Izquierdo 10/5/y 11:27

Supprimé:

Guillermo Gea Izquierdo 7/5/y 17:13

Mis en forme: Non Exposant/ Indice

542 | growth trends, even if there are changes in WUE, would express sink limitation mostly
543 | related to hydraulic constraints (Peñuelas et al. 2011; Sala et al. 2012; Keenan et al.
544 | 2013). Often, the trees express a growth decline at those sites where there is an
545 | enhancement in long-term water stress that dominates species performance (e.g. Bigler
546 | et al. 2006; Piovesan et al. 2008; Gea-Izquierdo et al. 2014). In contrast, it has been
547 | observed under certain conditions that trees have increased growth with warming since
548 | the 1850s (Salzer et al. 2009; Gea-Izquierdo & Cañellas 2014). These studies suggest
549 | the existence of a positive effect of warming rather than that of CO₂ fertilization upon
550 | growth in forests where water stress is not the most limiting factor. Our study sites are
551 | located within the Northern limit of the Mediterranean Region, meaning that the two
552 | species studied occupy drier and warmer areas more to the South. The two species have
553 | different functional characteristics, e.g. oaks are anisohydric whereas pines tend to be
554 | isohydric. This confers them different capacities of adaptation to climate change, which
555 | means that they should play different roles in future stand dynamics. Our results express
556 | the existence of trade-offs in response to climate at different phenological periods. This
557 | is important since synergistic environmental stresses acting at different periods can
558 | trigger tree mortality (McDowell et al. 2013; Voltas et al. 2013). Model sensitivity
559 | analysis could be performed to discuss the influence of specific factors such as climate
560 | or [CO₂] causing instability in the climate-growth response (D'Arrigo et al. 2008;
561 | Boucher et al. 2014). However [CO₂] enhancement and climate warming are mixed in
562 | analysis performed using data from field studies, which can make the isolation of their
563 | effect problematic. The model can be applied using abundant dendrochronological data
564 | used to determine the site-dependent parameters. This would give much flexibility to
565 | investigate growth trends and forest performance in response to global change at a
566 | larger scale.

Guillermo Gea Izquierdo 7/5/y 17:13

Supprimé: is

Guillermo Gea Izquierdo 7/5/y 17:13

Supprimé: [

Guillermo Gea Izquierdo 7/5/y 17:13

Supprimé:]

570

571 **Conclusions**

572 By developing an original process-based model with carbon allocation relationships
573 explicitly expressed as functions of climate we accurately simulated gross primary
574 productivity and allocation of carbon to secondary growth in evergreen Mediterranean
575 forests. Different processes were modelled as functions of environmental variability,
576 including [CO₂] and climate. The studied forests expressed trade-offs in carbon
577 allocation to different plant compartments in response to stress in different seasons,
578 namely with low temperatures and a short photoperiod in winter, and with moisture
579 shortage in summer. We modelled a decreasing time trend in stomatal conductance,
580 which would suggest a partly active increase of iWUE in the forests studied. Interannual
581 variability in WUE followed closely that of iWUE. However, WUE exhibited a
582 decreasing trend at the site where we simulated a decrease in LAI and GPP in response
583 to a decrease in annual precipitation since the 1980s. Long-term GPP remained at
584 similar levels in the last 50 years just in one stand whereas it declined in the forest
585 suffering a reduction in precipitation. This suggests different acclimation processes at
586 the canopy level and in the pattern of allocation in response to enhanced xericity and
587 increasing [CO₂] levels, which could not counterbalance the negative effect of warming
588 just in the site where there was a simultaneous decrease in precipitation. Tree growth
589 was partly decoupled from stand productivity, highlighting that it can be risky to accept
590 growth as a direct proxy to GPP. The model is flexible enough to assess both C-source
591 and C-sink limitations and includes a dynamic estimation of stored C. These features
592 would improve ecosystem models with a fixed C-source formulation. By calibrating a
593 limited number of parameters related to carbon allocation the model has great potential
594 to be used with abundant dendroecological data to characterise past instability in the

Guillermo Gea Izquierdo 7/5/y 17:13
Mis en forme: Non Exposant/ Indice

Guillermo Gea Izquierdo 7/5/y 17:14
Mis en forme: Non Exposant/ Indice

Guillermo Gea Izquierdo 10/5/y 11:31
Supprimé: one

596 growth response in relation to environmental variability and simulate future forest
597 response under different climatic scenarios.

598

599 **Acknowledgements**

600 G.G.I was funded by the Labex OT-Med (n° ANR-11-LABEX-0061) from the
601 «Investissements d’Avenir» program of the French National Research Agency through
602 the A*MIDEX project (n° ANR-11-IDEX-0001-02). Federation de Recherche FR3098
603 ECCOREV, the labex IRDHEI and OHM-BMP also supported the study. We are
604 grateful to Roland Huc for sharing data from Fontblanche.

605

606 **References**

- 607 Allard, V., Ourcival, J. M., Rambal, S., Joffre, R. and Rocheteau, A.: Seasonal and
608 annual variation of carbon exchange in an evergreen Mediterranean forest in
609 southern France, *Glob. Chang. Biol.*, 14(4), 714–725, 2008.
- 610 Baldocchi DD: Assessing the eddy covariance technique for evaluating carbon dioxide
611 exchange rates of ecosystems: Past, present and future. *Glob. Chang. Biol.*, 9, 479–
612 492, 2003.
- 613 Baldocchi, D. D., Ma, S. Y., Rambal, S., Misson, L., Ourcival, J. M., Limousin, J. M.,
614 Pereira, J. and Papale, D.: On the differential advantages of evergreenness and
615 deciduousness in mediterranean oak woodlands: a flux perspective, *Ecol. Appl.*,
616 20(6), 1583–1597, 2010.
- 617 Beer, C., Ciais, P., Reichstein, M., Baldocchi, D., Law, B. E., Papale, D., Soussana, J.-
618 F., Ammann, C., Buchmann, N., Frank, D., Gianelle, D., Janssens, I. a., Knohl, a.,
619 Köstner, B., Moors, E., Rouspard, O., Verbeeck, H., Vesala, T., Williams, C. a. and

620 Wohlfahrt, G.: Temporal and among-site variability of inherent water use efficiency
621 at the ecosystem level, *Global Biogeochem. Cycles*, 23(2), 2009.

622 Bernacchi, C. J., Singaas, E. L., Pimentel, C., Portis, A. R. and Long, S. P.: Improved
623 temperature response functions for models of Rubisco-limited photosynthesis, *Plant*
624 *Cell Environ.*, 24(2), 253–259, 2001.

625 Bigler, C., Braker, O. U., Bugmann, H., Dobbertin, M. and Rigling, A.: Drought as an
626 inciting mortality factor in Scots pine stands of the Valais, Switzerland,
627 *Ecosystems*, 9(3), 330–343, 2006.

628 Boucher, É., Guiot, J., Hatté, C., Daux, V., Danis, P. -a. and Dussouillez, P.: An inverse
629 modeling approach for tree-ring-based climate reconstructions under changing
630 atmospheric CO₂ concentrations, *Biogeosciences*, 11(12), 3245–3258, 2014.

631 Breda, N., Huc, R., Granier, A. and Dreyer, E.: Temperate forest trees and stands under
632 severe drought: a review of ecophysiological responses, adaptation processes and
633 long-term consequences, *Ann. For. Sci.*, 63(6), 625–644, 2006.

634 Breshears, D. D., Myers, O. B., Meyer, C. W., Barnes, F. J., Zou, C. B., Allen, C. D.,
635 McDowell, N. G. and Pockman, W. T.: Tree die-off in response to global change-
636 type drought: mortality insights from a decade of plant water potential
637 measurements, *Front. Ecol. Environ.*, 7(4), 185–189, 2009.

638 Chen, G., Yang, Y. and Robinson, D.: Allocation of gross primary production in forest
639 ecosystems: allometric constraints and environmental responses. *New Phytol.*,
640 200(1176-1186), 2013.

641 D'Arrigo, R., Wilson, R., Liepert, B. and Cherubini, P.: On the “Divergence Problem”
642 in Northern Forests: A review of the tree-ring evidence and possible causes, *Glob.*
643 *Planet. Change*, 60(3-4), 289–305, 2008.

644 De Pury, D.G.G. and Farquhar, G.D.: Simple scaling of photosynthesis from leaves to
645 canopies without the errors of big-leaf models. *Plant Cell Environ.*, 20(5), 537–557,
646 1997.

647 De Kauwe, M. G., Medlyn, B. E., Zaehle, S., Walker, A. P., Dietze, M. C., Hickler, T.,
648 Jain, A. K., Luo, Y. Q., Parton, W. J., Prentice, I. C., Smith, B., Thornton, P. E.,
649 Wang, S. S., Wang, Y. P., Warlind, D., Weng, E. S., Crous, K. Y., Ellsworth, D. S.,
650 Hanson, P. J., Seok Kim, H., Warren, J. M., Oren, R. and Norby, R. J.: Forest water
651 use and water use efficiency at elevated CO₂: a model-data intercomparison at two
652 contrasting temperate forest FACE sites, *Glob. Chang. Biol.*, 19(6), 1759–1779,
653 2013.

654 Dickman, L. T., McDowell, N. G., Sevanto, S., Pangle, R. E. and Pockman, W. T.:
655 Carbohydrate dynamics and mortality in a piñon-juniper woodland under three
656 future precipitation scenarios., *Plant. Cell Environ.*, 2014.

657 Evans, M. N., Reichert, B. K., Kaplan, A., Anchukaitis, K. J., Vaganov, E. A., Hughes,
658 M. K. and Cane, M. A.: A forward modeling approach to paleoclimatic
659 interpretation of tree-ring data, *J. Geophys. Res.*, 111(G3), 2006.

660 Farquhar, G.D., von Caemmerer, S. and Berry, J.A.: A biochemical model of
661 photosynthetic CO₂ assimilation in leaves of C₃ species, *Planta*, 149(1), 78–90,
662 1980.

663 Fatichi, S., Leuzinger, S. and Körner, C.: Moving beyond photosynthesis : from carbon
664 source to sink-driven vegetation modeling, *New Phytol.*, 201, 1086–1095, 2013.

665 Flexas, J., Bota, J., Galmes, J., Medrano, H. and Ribas-Carbo, M.: Keeping a positive
666 carbon balance under adverse conditions: responses of photosynthesis and
667 respiration to water stress, *Physiol. Plant.*, 127(3), 343–352, 2006.

668 Friedlingstein, P., Joel, G., Field, C. B. and Fung, I. Y.: Toward an allocation scheme
669 for global terrestrial carbon models, *Glob. Chang. Biol.*, 5(7), 755–770, 1999.

670 Fritts, H.C.: *Tree Rings and Climate*. Blackburn Press, 567 p, 1976

671 Gaucherel, C., Campillo, F., Misson, L., Guiot, J. and Boreux, J. J.: Parameterization of
672 a process-based tree-growth model: Comparison of optimization, MCMC and
673 Particle Filtering algorithms, *Environ. Model. Softw.*, 23(10-11), 1280–1288, 2008.

674 Gea-Izquierdo, G., Mäkelä, A., Margolis, H., Bergeron, Y., Black, T. A., Dunn, A.,
675 Hadley, J., Kyaw Tha Paw U, Falk, M., Wharton, S., Monson, R., Hollinger, D. Y.,
676 Laurila, T., Aurela, M., McCaughey, H., Bourque, C., Vesala, T. and Berninger, F.:
677 Modeling acclimation of photosynthesis to temperature in evergreen conifer forests.
678 *New Phytol.*, 188(1), 175–186, 2010.

679 Gea-izquierdo, G., Fernández-de-uña, L., Cañellas, I. Growth projections reveal local
680 vulnerability of Mediterranean oaks with rising temperatures. *For. Ecol. Manage.*,
681 305, 282–293, 2013.

682 Gea-Izquierdo, G. and Cañellas, I.: Long-term climate forces instability in long-term
683 productivity of a Mediterranean oak along climatic gradients. *Ecosystems*, 17, 228–
684 241, 2014.

685 Gea-Izquierdo, G., Viguera, B., Cabrera, M., Cañellas, I. Drought induced decline could
686 portend widespread oak mortality at the xeric ecotone in managed Mediterranean
687 pine-oak woodlands. *Forest Ecol. Manag.* 320, 70-82, 2014.

688 Granier, A., Breda, N., Longdoz, B., Gross, P. and Ngao, J.: Ten years of fluxes and
689 stand growth in a young beech forest at Hesse, North-eastern France, *Ann. For. Sci.*,
690 64 (7), 704, 2008.

691 Grassi, G. and Magnani, F.: Stomatal, mesophyll conductance and biochemical
692 limitations to photosynthesis as affected by drought and leaf ontogeny in ash and
693 oak trees, *Plant, Cell Environ.*, 28(7), 834–849, 2005.

694 Guiot, J., Boucher, E. and Gea-Izquierdo, G.: Process models and model-data fusion in
695 dendroecology, *Front. Ecol. Evol.*, 2(August), 1–12, 2014.

696 Hoff, C. and Rambal, S.: An examination of the interaction between climate, soil and
697 leaf area index in a *Quercus ilex* ecosystem, *Ann. For. Sci.*, 60(2), 153–161, 2003.

698 IPCC. Climate Change: The Physical Science Basis. Summary for policymakers.
699 Stocker, T.F. et al. (Eds.) IPCC, Geneva, Switzerland. pp 33. 2013.

700 Keenan, T., Maria Serra, J., Lloret, F., Ninyerola, M. and Sabate, S.: Predicting the
701 future of forests in the Mediterranean under climate change, with niche- and
702 process-based models: CO₂ matters!, *Glob. Chang. Biol.*, 17(1), 565–579, 2011.

703 Keenan, T. F., Hollinger, D. Y., Bohrer, G., Dragoni, D., Munger, J. W., Schmid, H. P.
704 and Richardson, A. D.: Increase in forest water-use efficiency as atmospheric
705 carbon dioxide concentrations rise., *Nature*, 499(7458), 324–7, 2013.

706 Koenig, W. D. and Knops, M. H.: Patterns of annual seed production by Northern
707 Hemisphere trees: a global perspective., *Am. Nat.*, 155(1), 59–69, 2000.

708 Körner, C., Basel, M.L. Growth Controls Photosynthesis – Mostly. *Nova Acta*
709 *Leopoldina*, 283, 273–283, 2013.

710 Leonardi, S., Gentilella, T., Guerrieri, R., Ripullone, F., Magnani, F., Mencuccini, M.,
711 Noije, T. V and Borghetti, M.: Assessing the effects of nitrogen deposition and
712 climate on carbon isotope discrimination and intrinsic water-use efficiency of
713 angiosperm and conifer trees under rising CO₂ conditions, *Glob. Chang. Biol.*,
714 18(9), 2925–2944, 2012.

715 Le Roux, X., Lacoite, A., Escobar-Gutierrez, A. and Le Dizes, S.: Carbon-based
716 models of individual tree growth: A critical appraisal, *Ann. For. Sci.*, 58(5), 469–
717 506, 2001.

718 Leuning, R.: A critical appraisal of a combined stomatal-photosynthesis model for C3
719 plants. *Plant Cell Environ.* 18, 339-355, 1995

720 Lévesque, M., Siegwolf, R., Saurer, M., Eilmann, B. and Rigling, A.: Increased water-
721 use efficiency does not lead to enhanced tree growth under xeric and mesic
722 conditions., *New Phytol.*, 203(1), 94–109, 2014.

723 Li, G., Harrison, S. P., Prentice, I. C. and Falster, D.: Simulation of tree ring-widths
724 with a model for primary production, carbon allocation and growth, *Biogeosciences*
725 *Discuss.*, 11(7), 10451–10485, 2014.

726 Limousin, J. M., Rambal, S., Ourcival, J. M., Rocheteau, A., Joffre, R. and Rodriguez-
727 Cortina, R.: Long-term transpiration change with rainfall decline in a Mediterranean
728 *Quercus ilex* forest, *Glob. Chang. Biol.*, 15(9), 2163–2175, 2009.

729 Limousin, J. M., Longepierre, D., Huc, R. and Rambal, S.: Change in hydraulic traits of
730 Mediterranean *Quercus ilex* subjected to long-term throughfall exclusion, *Tree*
731 *Physiol.*, 30(8), 1026–1036, 2010.

732 Limousin, J.-M., Rambal, S., Ourcival, J.-M., Rodriguez-Calcerrada, J., Perez-Ramos, I.
733 M., Rodriguez-Cortina, R., Misson, L. and Joffre, R.: Morphological and
734 phenological shoot plasticity in a Mediterranean evergreen oak facing long-term
735 increased drought, *Oecologia*, 169(2), 565–577, 2012.

736 Maseyk, K. S., Lin, T., Rotenberg, E., Grünzweig, J. M., Schwartz, A. and Yakir, D.:
737 Physiology-phenology interactions in a productive semi-arid pine forest., *New*
738 *Phytol.*, 178(3), 603–16, 2008.

739 McDowell, N.G., Fisher, R.A., Xu, C., Domec, J., Höltta, T., Mackay, D.S., Sperry, J.
740 S., Boutz, A., Dickman, L., Gehres, N., Limousin, J.M., Macalady, A., Pangle, R.
741 E., Rasse, D.P., Ryan, M.G., Sevanto, S., Waring, R.H., Williams, A.P., Yezpez, E.
742 A. and Pockman, W.T.: Evaluating theories of drought-induced vegetation mortality
743 using a multimodel – experiment framework, *New Phytol.*, 200, 304–321, 2013.

744 McMurtrie, R. E. and Dewar, R. C.: New insights into carbon allocation by trees from
745 the hypothesis that annual wood production is maximized, *New Phytol.*, 199(4),
746 981–990, 2013.

747 Millard, P., Sommerkorn, M., Grelet, G.A. Environmental change and carbon limitation
748 in trees: A biochemical, ecophysiological and ecosystem appraisal. *New*
749 *Phytologist*, 175, 11–28, 2007.

750 Misson, L.: MAIDEN: a model for analyzing ecosystem processes in dendroecology.
751 *Can. J. For. Res.*, 34, 874–887, 2004.

752 Misson, L., Rathgeber, C. and Guiot, J.: Dendroecological analysis of climatic effects
753 on *Quercus petraea* and *Pinus halepensis* radial growth using the process-based
754 MAIDEN model, *Can. J. For. Res.*, 34(4), 888–898, 2004.

755 Misson, L., Tang, J., Xu, M., Mckay, M. and Goldstein, A.: Influences of recovery from
756 clear-cut , climate variability , and thinning on the carbon balance of a young
757 ponderosa pine plantation, *Agric. Fore*, 130, 207–222, 2005.

758 Misson, L., Degueldre, D., Collin, C., Rodriguez, R., Rocheteau, A., Ourcival, J.-M.
759 and Rambal, S.: Phenological responses to extreme droughts in a Mediterranean
760 forest, *Glob. Chang. Biol.*, 17(2), 1036–1048, 2011.

761 Montserrat-Marti, G., Camarero, J. J., Palacio, S., Perez-Rontome, C., Milla, R.,
762 Albuixech, J. and Maestro, M.: Summer-drought constrains the phenology and
763 growth of two coexisting Mediterranean oaks with contrasting leaf habit:

764 implications for their persistence and reproduction, *Trees-Structure Funct.*, 23(4),
765 787–799, 2009.

766 Niinemets, U.: Photosynthesis and resource distribution through plant canopies., *Plant*
767 *Cell Environ.*, 30(9), 1052–71, 2007.

768 Niinemets, U. and Valladares, F.: Photosynthetic acclimation to simultaneous and
769 interacting environmental stresses along natural light gradients: optimality and
770 constraints., *Plant Biol. (Stuttg.)*, 6(3), 254–68, 2004.

771 Niinemets, Ü., Tenhunen, J. D., Canta, N. R., Chaves, M. M., Faria, T., Pereira, J. S.
772 and Reynolds, J. F.: Interactive effects of nitrogen and phosphorus on the
773 acclimation potential of foliage photosynthetic properties of cork oak, *Q. suber*, to
774 elevated atmospheric CO₂ concentrations, *Glob. Chang. Biol.*, 5, 455–470, 1999.

775 Nobel, P.S.: *Physicochemical and environmental plant physiology*. 4th edn. Academic
776 Press, Elsevier, Oxford UK, 2009.

777 Peng, C. H., Guiot, J., Wu, H. B., Jiang, H. and Luo, Y. Q.: Integrating models with
778 data in ecology and palaeoecology: advances towards a model-data fusion
779 approach, *Ecol. Lett.*, 14(5), 522–536, 2011.

780 Peñuelas, J., Hunt, J. M., Ogaya, R. and Jump, A. S.: Twentieth century changes of tree-
781 ring delta C-13 at the southern range-edge of *Fagus sylvatica*: increasing water-use
782 efficiency does not avoid the growth decline induced by warming at low altitudes,
783 *Glob. Chang. Biol.*, 14(5), 1076–1088, 2008.

784 Peñuelas, J., Canadell, J. G. and Ogaya, R.: Increased water-use efficiency during the
785 20th century did not translate into enhanced tree growth, *Glob. Ecol. Biogeogr.*,
786 20(4), 597–608, 2011.

787 Pereira, J. S., Mateus, J. A., Aires, L. M., Pita, G., Pio, C., David, J. S., Andrade, V.,
788 Banza, J., David, T. S., Paco, T. A. and Rodrigues, A.: Net ecosystem carbon

789 exchange in three contrasting Mediterranean ecosystems - the effect of drought,
790 Biogeosciences, 4(5), 791–802, 2007.

791 Pérez-Ramos, I. M., Ourcival, J. M., Limousin, J. M. and Rambal, S.: Mast seeding
792 under increasing drought: results from a long-term data set and from a rainfall
793 exclusion experiment, Ecology, 91(10), 3057–3068, 2010.

794 Piovesan, G., Biondi, F., Di Filippo, A., Alessandrini, A. and Maugeri, M.: Drought-
795 driven growth reduction in old beech (*Fagus sylvatica* L.) forests of the central
796 Apennines, Italy, Glob. Chang. Biol., 14(6), 1265–1281, 2008.

797 Rambal, S., Joffre, R., Ourcival, J. M., Cavender-Bares, J. and Rocheteau, a.: The
798 growth respiration component in eddy CO₂ flux from a *Quercus ilex* mediterranean
799 forest, Glob. Chang. Biol., 10(9), 1460–1469, 2004.

800 Reichstein, M., Tenhunen, J. D., Rouspard, O., Ourcival, J. M., Rambal, S., Miglietta,
801 F., Peressotti, A., Pecchiari, M., Tirone, G. and Valentini, R.: Severe drought effects
802 on ecosystem CO₂ and H₂O fluxes at three Mediterranean evergreen sites: revision
803 of current hypotheses?, Glob. Chang. Biol., 6(10), 999–1017, 2002.

804 Reichstein, M., Tenhunen, J., Rouspard, O., Ourcival, J. M., Rambal, S., Miglietta, F.,
805 Peressotti, A., Pecchiari, M., Tirone, G. and Valentini, R.: Inverse modeling of
806 seasonal drought effects on canopy CO₂/H₂O exchange in three Mediterranean
807 ecosystems, J. Geophys. Res., 108(23), 2003.

808 Reichstein, M., Falge, E., Baldocchi, D., Papale, D., Aubinet, M., Berbigier, P.,
809 Bernhofer, C., Buchmann, N., Gilmanov, T., Granier, A., Gruhnwald, T.,
810 Havranekova, K., Ilvesniemi, H., Janous, D., Knohl, A., Laurila, T., Lohila,
811 A., Loustau, D., Matteucci, G., Meyers, T., Miglietta, F., Ourcival, J. M.,
812 Pumpanen, J., Rambal, S., Rotenberg, E., Sanz, M., Tenhunen, J., Seufert, G.,
813 Vaccari, F., Vesala, T., Yakir, D. and Valentini, R.: On the separation of net

814 ecosystem exchange into assimilation and ecosystem respiration: Review and
815 improved algorithm, *Glob. Chang. Biol.*, 11(9), 1424–1439, 2005.

816 Sala, A. and Tenhunen, J. D.: Simulations of canopy net photosynthesis and
817 transpiration in *Quercus ilex* L. under the influence of seasonal drought, *Agric. For.*
818 *Meteorol.*, 78 203–222, 1996.

819 Sala, A., Woodruff, D. R. and Meinzer, F. C.: Carbon dynamics in trees: feast or
820 famine?, *Tree Physiol.*, 32(6), 764–75, 2012.

821 Salzer, M. G., Hughes, M. K., Bunn, A. G. and Kipfmüller, K. F.: Recent
822 unprecedented tree-ring growth in bristlecone pine at the highest elevations and
823 possible causes., *PNAS*, 106(48), 20348–20353, 2009.

824 Saurer, M., Spahni, R., Frank, D.C., Joos, F., Leuenberger, M., Loader, N.J., McCarroll,
825 D., Gagen, M., Poulter, B., Siegwolf, R. T. W., Andreu-Hayles, L., Boettger, T.,
826 Dorado, I., Fairchild, I. J., Friedrich, M., Gutierrez, E., Haupt, M., Hiltunen, E.,
827 Heinrich, I., Helle, G., Grubb, H., Jalkanen, R., Levanič, T., Linderholm, H. W.,
828 Robertson, I., Sonninen, E., Treydte, K., Waterhouse, J. S., Woodley, E. J., Wynn,
829 P. M. and Young, G. H. F.: Spatial variability and temporal trends in water-use
830 efficiency of European forests., *Glob. Chang. Biol.*, 3700–3712, 2014.

831 Schaefer, K., Schwalm, C.R., Williams, C., Arain, M.A., Barr, A., Chen, J.M., Davis,
832 K. J., Dimitrov, D., Hilton, T.W., Hollinger, D.Y., Humphreys, E., Poulter, B.,
833 Raczka, B.M., Richardson, A.D., Sahoo, A., Thornton, P., Vargas, R., Verbeeck,
834 H., Anderson, R., Baker, I., Black, T.A., Bolstad, P., Chen, J., Curtis, P.S., Desai,
835 A. R., Dietze, M., Dragoni, D., Gough, C., Grant, R. F., Gu, L., Jain, A., Kucharik,
836 C., Law, B., Liu, S., Lokipitiya, E., Margolis, H.A., Matamala, R., McCaughey, J.
837 H., Monson, R., Munger, J.W., Oechel, W., Peng, C., Price, D. T., Ricciuto, D.,
838 Riley, W. J., Roulet, N., Tian, H., Tonitto, C., Torn, M., Weng, E. and Zhou, X.: A

839 model-data comparison of gross primary productivity: Results from the North
840 American Carbon Program site synthesis, *J. Geophys. Res.*, 117(G3), G03010,
841 2012.

842 Simioni, G., Durand-Gillmann, M. and Huc, R.: Asymmetric competition increases leaf
843 inclination effect on light absorption in mixed canopies, *Ann. For. Sci.*, 70(2), 123–
844 131, 2013.

845 Sun, Y., Gu, L., Dickinson, R. E., Norby, R. J., Pallardy, S. G. and Hoffman, F. M.:
846 Impact of mesophyll diffusion on estimated global land CO₂ fertilization, *Proc.*
847 *Natl. Acad. Sci. U. S. A.*, 111(44), 15774–15779, 2014.

848 Tolwinski-Ward, S. E., Evans, M. N., Hughes, M. K. and Anchukaitis, K. J.: An
849 efficient forward model of the climate controls on interannual variation in tree-ring
850 width, *Clim. Dyn.*, 36(11-12), 2419–2439, 2011.

851 Touchan, R., Shishov, V. V., Meko, D. M., Nouiri, I. and Grachev, A.: Process based
852 model sheds light on climate sensitivity of Mediterranean tree-ring width,
853 *Biogeosciences*, 9(3), 965–972, 2012.

854 Vaganov, E.A., Hughes, M.K., Shashkin, A.V. *Growth Dynamics of Conifer Tree*
855 *Rings: Images of Past and Future Environments*. Springer, New York. 2006.

856 Vaz, M., Pereira, J. S., Gazarini, L. C., David, T. S., David, J. S., Rodrigues, A.,
857 Maroco, J. and Chaves, M. M.: Drought-induced photosynthetic inhibition and
858 autumn recovery in two Mediterranean oak species (*Quercus ilex* and *Quercus*
859 *suber*), *Tree Physiol.*, 30(8), 946–956, 2010.

860 Voltas, J., Camarero, J. J., Carulla, D., Aguilera, M., Ortiz, A. and Ferrio, J. P.: A
861 retrospective, dual-isotope approach reveals individual predispositions to winter-
862 drought induced tree dieback in the southernmost distribution limit of Scots pine.,
863 *Plant. Cell Environ.*, 36(8), 1435–48, 2013.

864 **Table 1.** Characteristics of mean annual gross primary productivity, climatic (annual
865 means) and growth data. Standard deviations are shown between parentheses.
866 Precipitation=mean annual precipitation; Tmax=annual mean of mean daily maximum
867 temperature; Tmin= annual mean of mean daily minimum temperature.
868 Length=chronology year replicated with more than 5 radii; RW=mean annual ring-
869 width; Rbs = mean correlation between series; AR = mean autocorrelation of raw series;
870 MS = mean sensitivity; EPS = mean expressed population signal Rbs, AR, MS and EPS
871 are classical statistics to characterise growth chronologies, and follow Fritts (1976).

872

		Fontblanche		Puechabon
Flux Data	Period	2008-2012		2001-2013
	GPP annual (g C m ⁻² year ⁻¹)	1431.4 (305.4)		1207.3 (206.7)
Climate	Period	1964-2012		1954-2013
	Precipitation (mm)	642.7 (169.7)		1002.6 (328.2)
	Tmax (°C)	20.6 (0.9)		17.8 (1.26)
	Tmin (°C)	8.8 (0.5)		8.1 (0.8)
Growth Data	Species	<i>P. halepensis</i>	<i>Q. ilex</i>	<i>Q. ilex</i>
	# Trees/Radii	25/47	15/30	17/32
	Length	1910-2013	1941-2013	1941-2005
	RW (mm)	2.19 (1.1)	1.25 (0.7)	1.13 (0.7)
	MS	0.308	0.372	0.443
	AR	0.684	0.591	0.436
	EPS	0.541	0.281	0.457
		0.963	0.884	0.949

873

874 **Table 2.** Model parameters. Those parameter differing between sites were optimized
875 either with GPP data (photosynthesis and allocation module) or with growth-based
876 biomass increment chronologies (allocation module). The rest were common parameters
877 for both sites and selected while developing the model in the first step for Fontblanche
878 using GPP data (represented in ‘Cal’ with a ‘-’). Meaning of parameters, equation
879 number (E#) and phenophase [P#] are as in the text in Material and Methods.
880 Fontb=Fontblanche; Puech=Puechabon; Cal=local parameters to be calibrated with GPP
881 or stem biomass increment data (SBI).

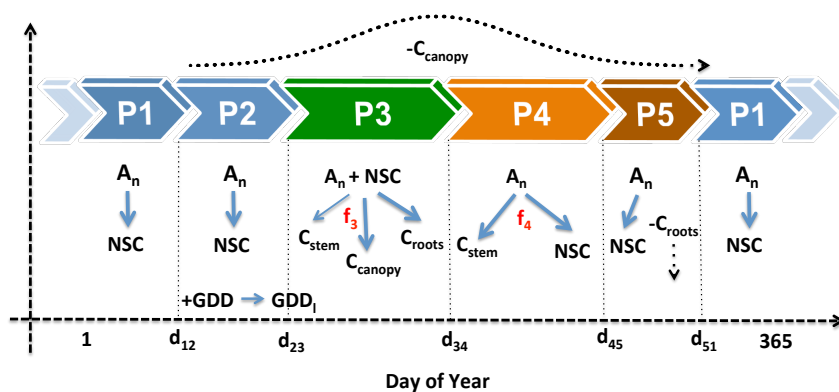
882

Process	Process/Equation #	Parameter	Fontb	Puech	Units	Cal	
Photosynthesis	Leaf photosynthesis [E2]	J_{coef}	QUIL	1.59		$\mu\text{mol C m}^{-2} \text{s}^{-1}$	-
		PIHA	1.44	-			
	Leaf photosynthesis [E3]	V_{max}	QUIL	32.3		$\mu\text{mol C m}^{-2} \text{s}^{-1}$	-
			PIHA	46.0	-		
		V_b	QUIL	-0.106		$^{\circ}\text{C}^{-1}$	-
			PIHA	-0.180	-		
	V_{ip}	QUIL	13.7		$^{\circ}\text{C}$	-	
		PIHA	20.0	-			
	Stress V_{cmax} [E4]	p_{str}	-0.05		mm^{-1}	-	
	Stomatal conductance [E5]	g_l	QUIL	7.5		-	-
PIHA			6.1	-			
	VPD_0	30000		Pa	-		
Water stress [E6]	$Soil_b$	-0.054		mm^{-1}	-		
	$Soil_{ip}$	22.2	81.8	mm	GPP		
Allocation	Respiration [E7]	p_{resp}	-0.225		$^{\circ}\text{C}^{-1}$	-	
	Stress LAI [E8]	p_{LAI}	65.5		mm	-	
	[P2]	GDD_l	203.3		$^{\circ}\text{C}$	-	
	Stored carbon buds [P3]	C_{bud}	7		g C day^{-1}	-	
	[P5]	Photoperiod	9.5		hours	-	
	Allocation canopy [P3], [E9]	st_{4moist}	-0.089	-0.173	mm^{-1}	GPP	
		st_{4temp}	53.3	75	$^{\circ}\text{C}$	GPP	
		st_{4sd}	26.9	26.1	$^{\circ}\text{C}$	GPP	
	Allocation stem [P3], [E10]	st_{3moist}	-0.045	-0.117	mm^{-1}	SBI	
		st_{3temp}	32.9	6.3	$^{\circ}\text{C}$	SBI	
		st_{3sd}	38.0	3.0	$^{\circ}\text{C}$	SBI	
Allocation stor/stem [P4], [E11]	st_{4moist}	200.8	119.3	mm	SBI		
	st_{4temp}	0.060	-0.097	$^{\circ}\text{C}^{-1}$	SBI		

883

884 **Figure 1.** Outline of the different phenological phases (P1 to P5) and carbon allocation
 885 in the model within a given year. A_n =net daily carbon assimilation; NSC=storage (non-
 886 structural carbohydrates); GDD=growing degree days, GDD_i =parameter determining
 887 shift from P2 to P3 (see text); C=carbon allocated either to the stem, canopy or roots;
 888 d=day of year. Solid arrows correspond to allocation within the plant whereas dashed
 889 arrows to correspond to litterfall (canopy or roots). f_3 and f_4 are nonlinear functions of
 890 soil water content and temperature determining carbon allocation to different
 891 compartments (see text for more details).

892



893 **Figure 2.** Growth (basal area increment, BAI, $\text{cm}^2 \cdot \text{year}^{-1}$) and biomass allocated to the
 894 tree stem ($\text{g C} \cdot \text{m}^{-2} \cdot \text{year}^{-1}$) of *Q. ilex* and *P. halepensis* at Fontblanche (growth shown in
 895 (a), biomass in (b)) and *Q. ilex* at Puechabon (growth and stem biomass shown in (c)).
 896 A vertical dashed line marks the release event in Fontblanche produced by the enhanced
 897 winter mortality in 1985 in (a). Dark lines for BAI correspond to yearly means while
 898 grey polygons show confidence intervals (at 95%) on the standard errors of the mean.

899

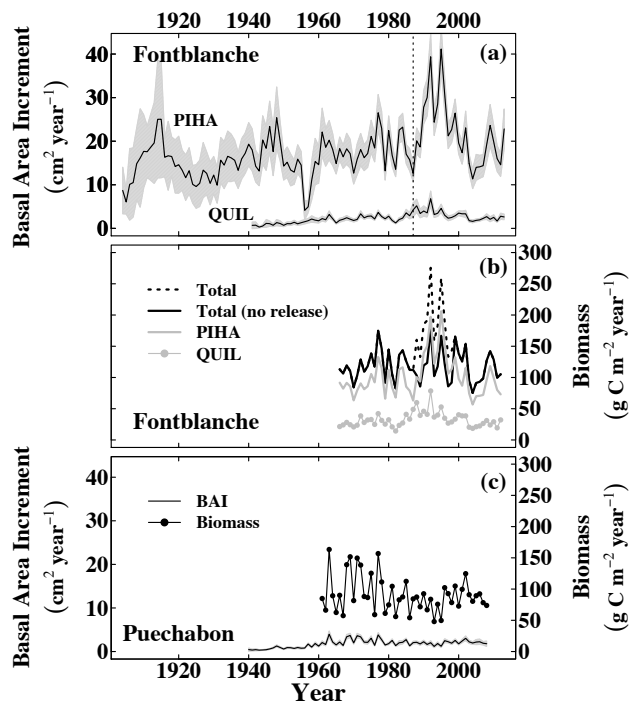


Figure 3. Daily gross primary productivity (GPP) at Puechabon (2001-2013, black dots, blue line) and Fontblanche (2008-2012, orange dots, red line). DOY=day of year. Thick lines correspond to smoothers fitted to the mean to highlight seasonal trends at the two sites.

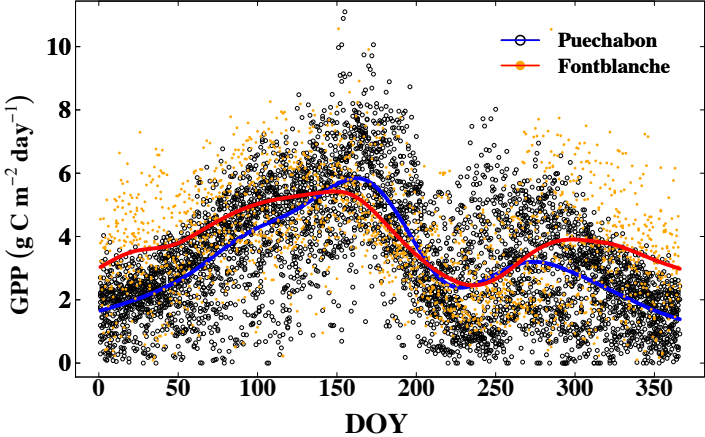


Figure 4. Model fit to stem biomass increment (a) and GPP (b) in Fontblanche; and stem biomass increment (c) and GPP (d) in Puechabon. R^2 =coefficient of determination; ρ =linear correlation between estimated and observed data, ρ_{low15} =linear correlation between estimated and observed data smoothed with a 15 year low-pass filter (blue and red lines in (b) and (c)). Polygons behind the estimated values in (a) and (c) correspond to confidence intervals of the mean: solid grey polygons for estimated values and dashed polygons for observed stem biomass increment values.

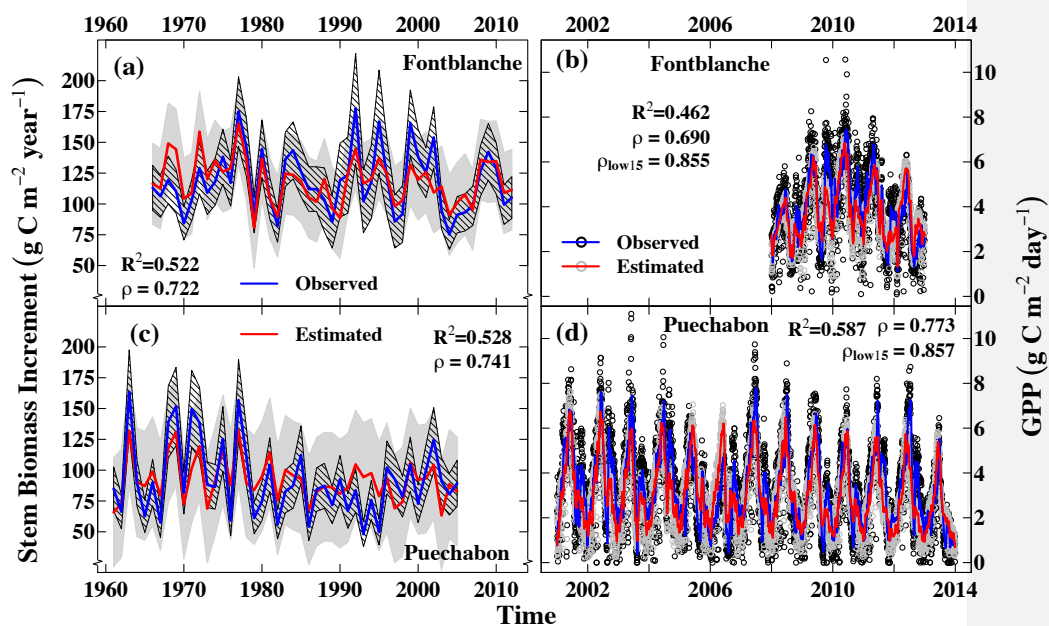


Figure 5. Modelled carbon allocation trajectory to the stem when leaf flush has finished in phenological period [P4]. We show the unitless modifier $1-h_4(i)$ (i.e. $h_4(i)$ is the portion of allocated carbon to storage) from $C_{stem}(i) = A_N(i) \cdot [(1-h_4(i))]$ as from [E11]. The modifier $[0,1]$ is a function of soil water content (SWC) and maximum temperature (T_{max}) and multiplies available daily carbon to distribute daily carbon allocated between secondary growth and storage.

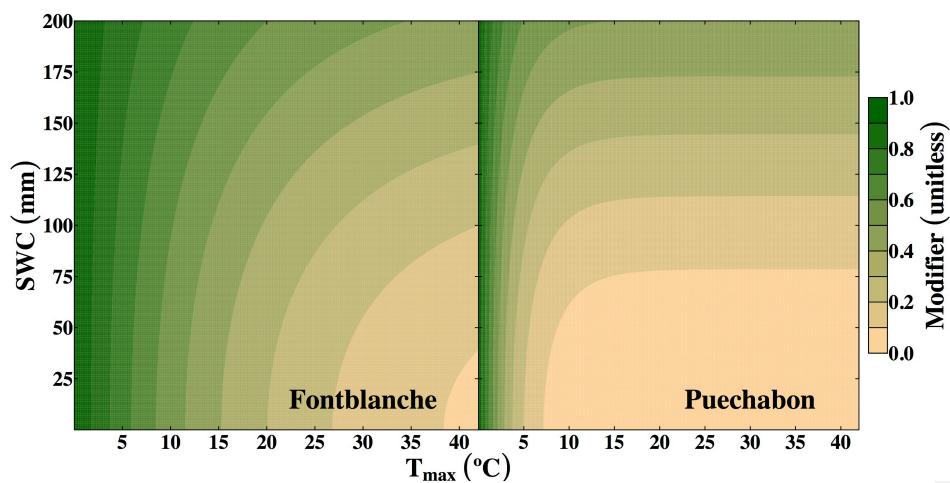
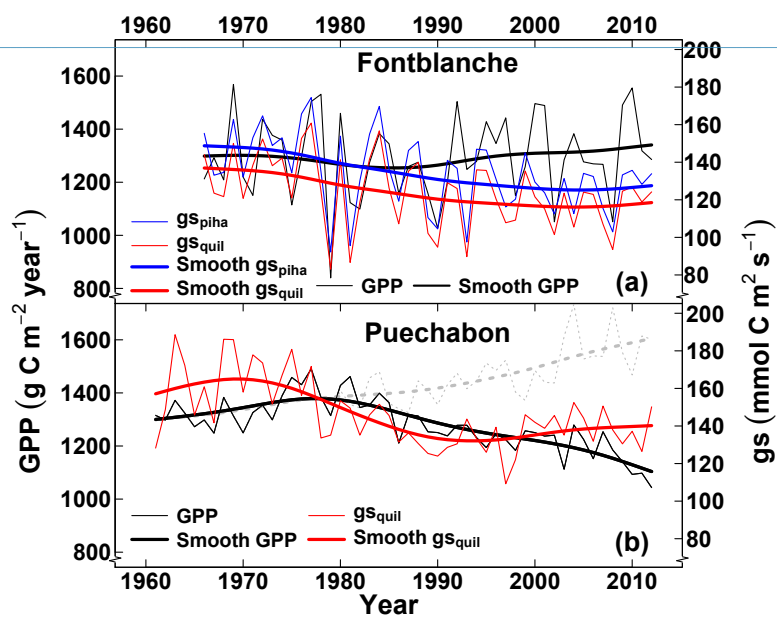


Figure 6. Modelled total annual stand gross primary productivity (GPP) and mean stomatal conductance of sunny leaves (gs) for Fontblanche (a) and Puechabon (b) for the period where meteorological data were available. [To show the influence of the precipitation decline observed in Puechabon on GPP we run a sensitivity simulation where precipitation was set fixed for 1980-2012 as in 1960-1979 \(Figure A1\) and all other input variables \(\$T_{min}\$, \$T_{max}\$, \$\[CO_2\]\$ \) were actual values. GPP values from this simulation are depicted as dashed grey lines in \(b\).](#)



Unknown
 Mis en forme: Police :(Par défaut) Times
 New Roman, 12 pt, Couleur de police :
 Automatique

Guillermo Gea Izquierdo 8/5/y 09:21
 Supprimé: <sp>

Unknown
 Mis en forme: Police :(Par défaut) Times
 New Roman, 12 pt, Couleur de police :
 Automatique

Figure 7. Ecosystem WUE (integral annual) and iWUE for sun leaves (mean daily, for PIHA and QUIL separated in Fontblanche) for (a) Fontblanche and (b) Puechabon for the period where we had available meteorological data.

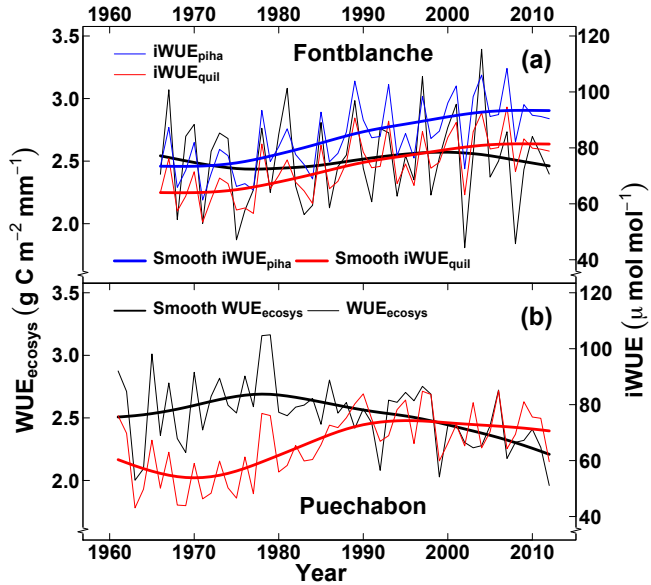


Figure A1. Mean climatic time series in the last 50 years. (a) annual precipitation; (b) and (c) annual maximum (Tmax) and minimum (Tmin) temperatures for Fontblanche (b) and Puechabon (c).

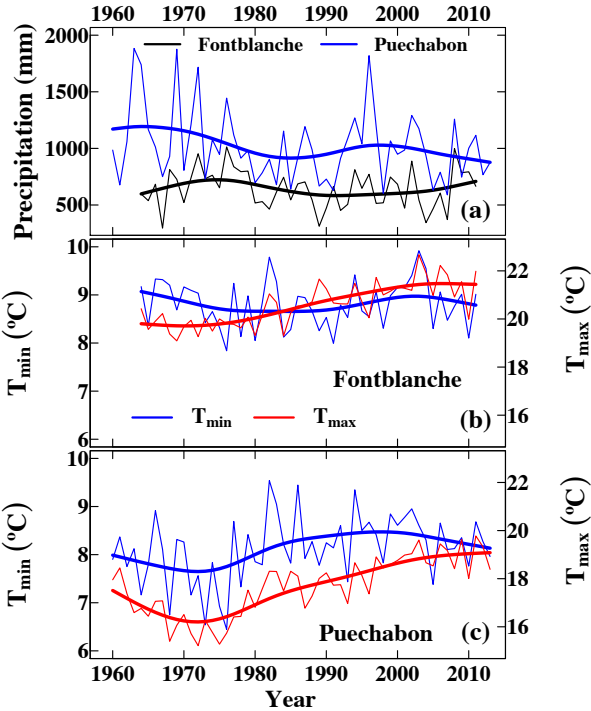


Figure A2. Diameter (dbh, cm) and age (years) distribution of trees included in the chronologies. Frequencies are calculated separately by species and site.

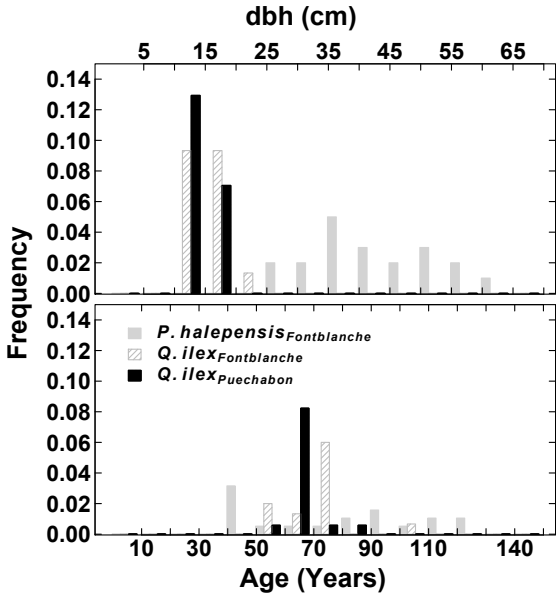


Figure A3. Simulated maximum annual leaf area index LAI ($\text{m}^2 \cdot \text{m}^{-2}$) and total annual stand transpiration E (mm/year) in Fontblanche (a) and Puechabon (b).

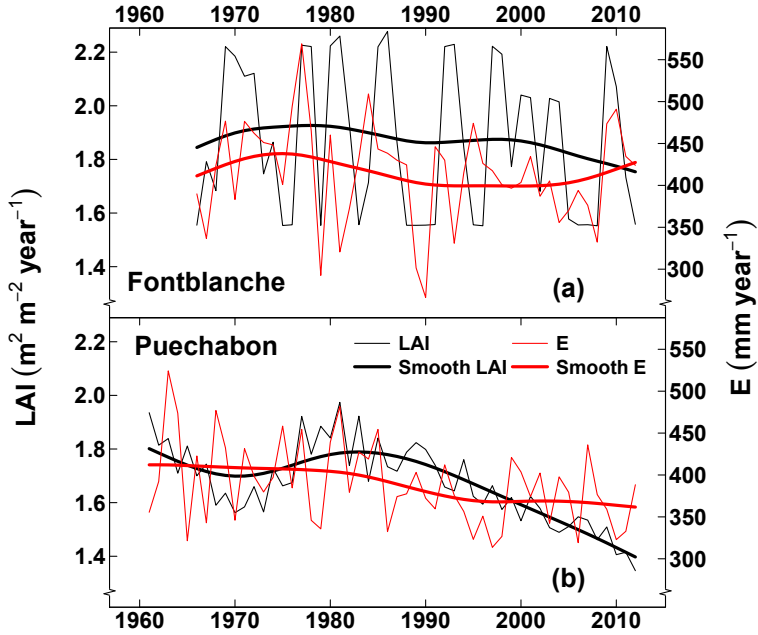


Figure A4. Simulated mean annual stomatal conductance (g_s) as a function of mean [CO₂] (a) and mean maximum temperature (b).

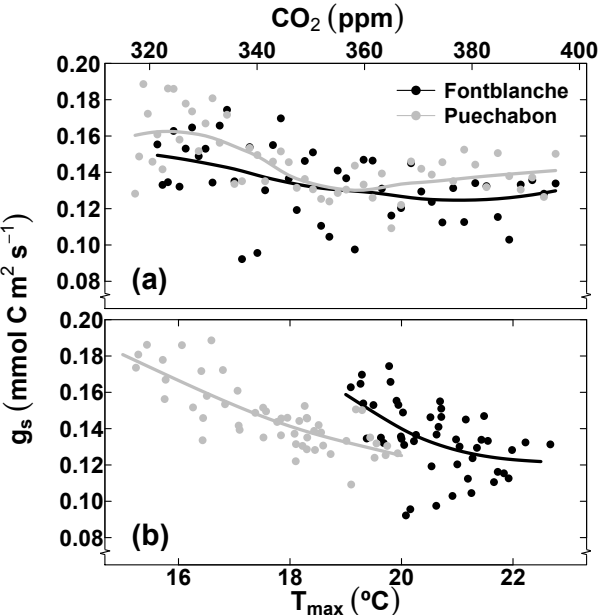
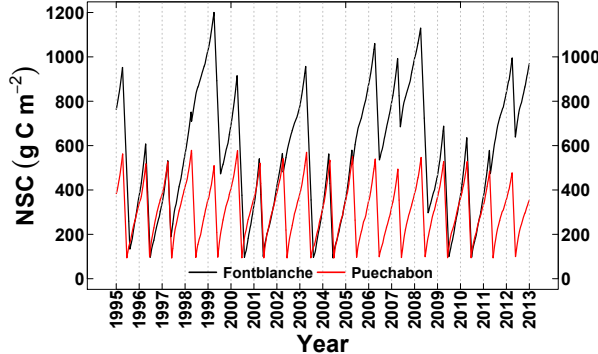


Figure A5. Simulated non-structural carbohydrate content (NSC) in the storage pool at both sites. The period 1995-2012 is shown to highlight within year variability.



Guillermo Gea Izquierdo 8/5/y 09:17
Mis en forme: Interligne : multiple 1.15 li